A Transient Heat and Mass Transfer Model of Residential Attics Used to Simulate Radiant Barrier Retrofits, Part I: Development

M. A. Medina
Assistant Professor,
Department of Mechanical and Industrial Engineering,
Texas A&M University-Kingsville,
Kingsville, TX 78363

D. L. O'Neal
Professor,
Department of Mechanical Engineering,
Texas A&M University,
College Station, TX 77843

W. D. Turner
Director,
Energy Systems Laboratory,
Texas Engineering Experiment Station,
College Station, TX 77843

This paper describes a transient heat and mass transfer model of residential attics. The model is used to predict hourly ceiling heat gain/loss in residences with the purpose of estimating reductions in cooling and heating loads produced by radiant barriers. The model accounts for transient conduction, convection, and radiation and incorporates moisture and air transport across the attic. Environmental variables, such as solar loads on outer attic surfaces and sky temperatures, are also estimated. The model is driven by hourly weather data which include: outdoor dry bulb air temperature, horizontal solar and sky radiation, wind speed and direction, relative humidity (or dew point), and cloud cover data. The output of the model includes ceiling heat fluxes, inner and outer heat fluxes from all surfaces, inner and outer surface temperatures, and attic dry bulb air temperatures. The calculated fluxes have been compared to experimental data of side-by-side testing of attics retrofit with radiant barriers. The model predicts ceiling heat flows with an error of less than ten percent for most cases.

Introduction

Year-long simulations of attic performance are important for determining the effects of design changes as well as retrofits on energy usage. Of special importance is the retrofit of installing radiant barriers inside attic spaces in combination with the existing attic insulation. Radiant barriers are thin metal sheets (usually aluminum) characterized by having at least one low emissivity surface (less than 0.05). Radiant barriers have received increased attention during the past decade because of their potential to reduce the radiant heat (from attic decks and gable ends) absorbed through the ceiling in a residence. Aluminum is used because it is inexpensive and because its surface is covered with a layer of a transparent oxide which protects it from the atmosphere and allows it to maintain its emissivity value unchanged for long periods of time. Engineering and economic models are needed to better understand the physical phenomena affecting the performance of radiant barriers as well as to make accurate economic assessments of savings produced by them. The success of any modeling effort depends upon the accuracy of the model, and the accuracy of the model depends on how well it captures the heat and mass transfer processes that occur in the attic.

The heat transfer in attic spaces is transient. The performance of attic systems is driven mainly by solar loads on the outer surfaces, outdoor temperatures, and wind which flow around the structure and vary throughout the day (Fig. 1). Therefore, in attic systems, all modes of heat transfer (transient conduction, natural and forced convection, and radiation) are present. In addition to the heat transfer problem, attics have an inflow and outflow of ventilating air and moisture which affect their performance. A model was developed which allowed instantaneous sensible and latent cooling and heating loads to be calculated based on energy balance equations written for each enclosing surface and for attic air layers. These equations were written in terms of unknown temperatures based on heat transfer processes (conduction, convection and/or radiation) which used previous temperatures and heat fluxes as well as physical descriptions of the attic components (*X-Y-Z* response factors). The model drew upon previously reported methodologies by Wilkes (1989, 1991) and Peavy (1979). A novel feature added by this model is the calculation of solar loads on all outer surfaces as a function of geographic location, house orientation, surface inclination, day of year, and hour of day. Earlier work assumed solar loads were independent of surface inclination. In addition, attic air stratification effects were incorporated instead of assuming that the attic air exists at one single temperature as referenced methodologies assumed.

Model Development

The attic used in the development of the model was a five-sided symmetrical attic composed of two pitched roof sections, two vertical gable-end sections, and one horizontal ceiling frame. The model followed the reasoning that at any attic surface, the heat flux entering through one side was equal to the heat flux leaving the opposite side plus the heat stored within the structure. For example, for a roof section facing the sun, the radiation heat flow from the sun minus the re-radiated flow from the roof minus the flow convected to the outdoor air was exactly balanced by the conductive flux leaving the roof section into the attic interior plus the heat stored within the attic deck. Equally, the conducted heat and the heat stored were balanced by the flow convected to the attic ventilating air plus the net radiation loss from the interior surface of this component. Thus for any surface, the heat balance equation was

$$Q_{\text{conducted(to/from)}} + \text{Heat Stored} + Q_{\text{convected(to/from)}} + Q_{\text{radiated(net)}} + Q_{\text{latent(condensation/evaporation)}} = 0 \quad (1)$$

Contributed by the Solar Energy Division of THE AMERICAN SOCIETY OF MECHANICAL ENGINEERS for publication in the ASME JOURNAL OF SOLAR ENERGY ENGINEERING. Manuscript received by the ASME Solar Energy Division, Mar. 1996; final revision, Feb. 1997. Associate Technical Editor: D. E. Claridge.

Stephenson, 1967), Equation (1) was expressed as

$$\sum_{j=0,j=1}^{N,S} Y_{i,j}(Tsi_{i,n\Delta-j} - Tr) - \sum_{j=0,j=1}^{N,S} X_{i,j}(Tso_{i,n\Delta-j} - Tr) + CR_i q''_{o(i,n\Delta-1)} + ho_i(T_{amb} - Tso_{i,n\Delta}) + hro_i(T_{sky/surr} - Tso_{i,n\Delta}) + \alpha q''_{sol,i} = 0 \quad (2)$$

for attic exterior surfaces, and as

$$\sum_{j=0,j=1}^{N,S} Z_{i,j}(Tsi_{i,n\Delta-j} - Tr) - \sum_{j=0,j=1}^{N,S} Y_{i,j}(Tso_{i,n\Delta-j} - Tr) + CR_i q''_{i(i,n\Delta-1)} + hi_i(Tsi_{i,n\Delta} - T_{attic\ air,n\Delta}) + \sum_{k=1,i=1}^{s,s} hri_{i,k}(Tsi_{i,n\Delta} - Tsi_{k,n\Delta}) + q''_{latent,i} = 0 \quad (3)$$

for attic interior surfaces, where

$$X_n = -\frac{k}{l}\frac{l^2}{\alpha\Delta}\left[\frac{2}{\pi^2}\sum_{m=1}^{\infty}\frac{\gamma_m^{n+1} - 2\gamma_m^n + \gamma_m^{n-1}}{m^2}\right] \quad (4)$$

$$Y_n = -\frac{k}{l}\frac{l^2}{\alpha\Delta}\left[\frac{2}{\pi^2}\sum_{m=1}^{\infty}\frac{(-1)^m(\gamma_m^{n+1} - 2\gamma_m^n + \gamma_m^{n-1})}{m^2}\right] \quad (5)$$

$$\gamma_m = e^{(-m^2\pi^2(\alpha\Delta/l^2))}. \quad (6)$$

According to Mitalas and Stephenson (1967), the response factors $X_{n,j}$ and $Z_{n,j}$ are the same. This is because of the symmetry of the slabs used to derive these factors. The multilayer walls found in building applications are assumed to be composed of

dure used to determine the heat fluxes at the surfaces layer components is used. A process of combination c layer response factors is repeated as many times as the of layers in a multilayer wall. Equations (4) and (5) w to estimate the response factors when the index n larger. Equations used to estimate X_o, Y_o, X_1 and Y_1 are in the Appendix.

Conduction Heat Transfer. Conduction heat tr attics occurs at all bounding surfaces and is a transient ena because the temperatures on all surfaces vary w For simplicity, each of the bounding surfaces of the approximated as one-dimensional transient conductio This approximation simplified the conduction problem valid under most circumstances unless metal framin metal supports were simulated (residential attic stru most instances, do not use metal framing nor metal s Heat fluxes were estimated using

$$q_{cond,out} = \sum_{j=0,j=1}^{N,S} Y_{i,j}(Tsi_{i,n\Delta-j} - Tr) - \sum_{j=0,j=1}^{N,S} X_{i,j}(Tso_{i,n\Delta-j} - Tr) + CR_i q''_{o(i,n}$$

for outgoing heat flux, and

$$q_{cond,in} = \sum_{j=0,j=1}^{N,S} Z_{i,j}(Tsi_{i,n\Delta-j} - Tr) - \sum_{j=0,j=1}^{N,S} Y_{i,j}(Tso_{i,n\Delta-j} - Tr) + CR_i q''_{i(i,n}$$

Nomenclature

A = surface area
B = radiosity
a, b, c, d, e = constants
C_p = specific heat at constant pressure
CR = common ratio
D_v = mass diffusivity
EW = equivalent width
F = shape factor
G = radiation coefficient
h, hi, ho = heat transfer coefficient
h_{fg} = latent heat of vaporization
hri, hro = radiation heat transfer coefficients
HRB = horizontal radiant barrier
I = irradiation
k = thermal conductivity
l, L = length, characteristic length
$\dot{m}$ = mass flow rate
n = cloud cover fraction, index
Nu = Nusselt number
P = pressure
Perm = permeability
Pr = Prantl number
Q = heat flow, volumetric flowrate
q'' = heat flux
R = thermal resistance
Ra = Rayleigh number
Re = Reynolds number
T = temperature
t = time
Tr = reference temperature
TRB = truss radiant barrier
Tsi = inside surface temperature
Tso = outside surface temperature
u = moisture content of wood
V = velocity
W = width
w = humidity ratio
X, Y, Z = response factors

Greek Symbols

α = thermal diffusivity, solar absorptivity
β = volumetric expansion, tilt angle
χ = radiation matrix
δ = kroneker delta, declination angle
Δ = time increment
ϵ = thermal emissivity
ϕ = angle, latitude, relative humidity
Γ = cloud emissivity factor
γ = surface azimuth angle
μ = dynamic viscosity
ν = kinematic viscosity
π = 3.141592
θ = incidence angle
ρ = density
σ = Stefan-Boltzman constant
τ = time
Ω = emissive power
ω = hour angle
ψ = inverse of χ mat

Subscripts

0, 1, 2, . . . = time denoting in (response factors
amb = ambient conditio
b = beam
cond = conductive
conv = convective
d = diffuse
D1, D2 = deck sections
dp = dew point
f = attic floor
F = forced
G1, G2 = gable sections
HOR = horizontal
i = denotes surface, indoor condition
j = denotes time, in
k = denotes surface
N = natural
$n\Delta$ = time step
o = outdoor conditio
rad = radiative
w = wood
x = local

Index

N = Number of surfa
S = Number of time

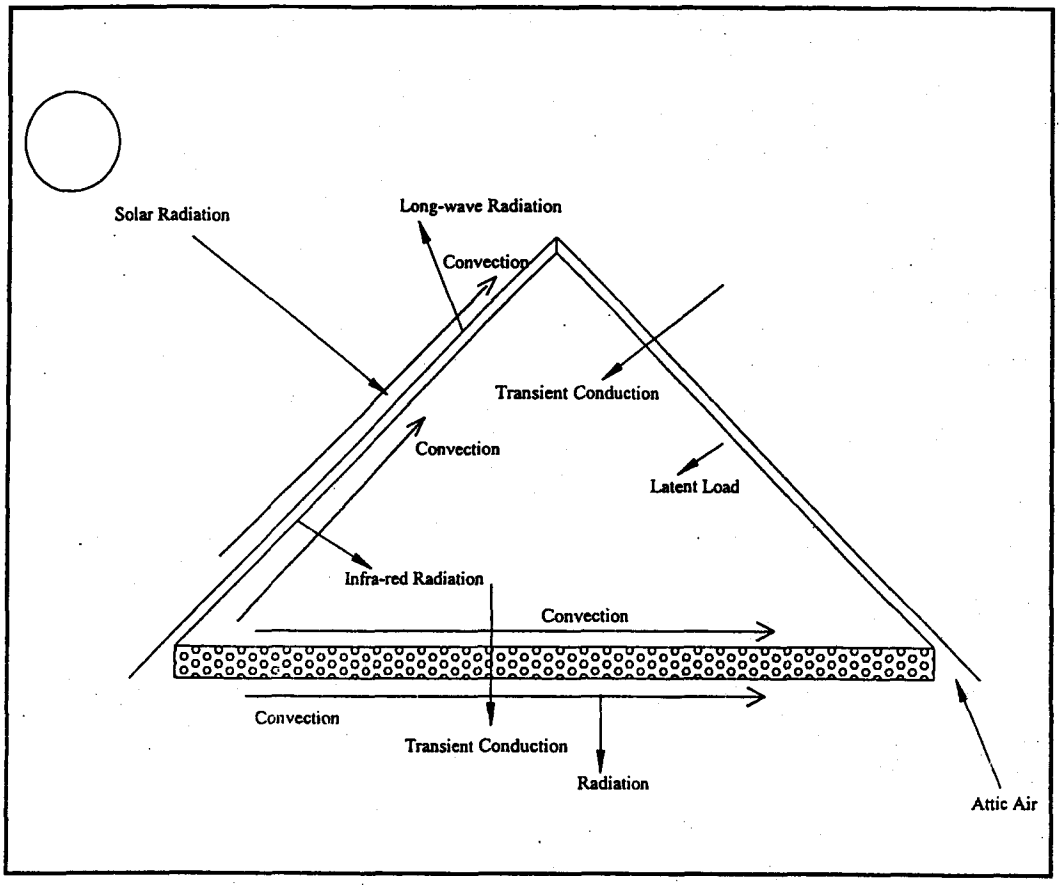

Fig. 1 Attic heat and mass transfer processes

for incoming heat flux. Equations (4) through (6) describe the parameters used in Eqs. (7) and (8).

Wood joists were accounted for in the estimation of the X, Y, and Z response factors. This was accomplished via area weighted values for the conduction parameters. In the "Validation Section" (accompanying paper, Part II), measured heat fluxes also accounted for wood joists as part of the ceiling frame.

Convection Heat Transfer. Attic ventilation is used to reduce excessive attic temperatures during the summertime and to lessen moisture accumulation during winter. At every surface, convection heat transfer can be significant. In this model, attic ventilation was simulated as forced ventilation. During a typical summer day, heat is transported away from outer surfaces by convection to the wind which flows around the structure, also the attic ventilating air carries away heat which otherwise would end up in the conditioned space. Convection in attics is mixed, meaning that both the effects of buoyancy forces as well as the effects of forced flows are present. Convection in attics can be laminar or turbulent, depending on the conditions present at a particular surface in question. Churchill (1977) proposed that the local Nusselt number in mixed convection be a combination of the local Nusselt number for forced convection and the local Nusselt number for natural convection for the same geometry. In equation form,

$$\mathrm{Nu}_x^n = \mathrm{Nu}_F^n \pm \mathrm{Nu}_N^n. \quad (9)$$

Chen et al. (1986) suggested that Churchill's correlation could also be applied to the average mixed convection Nusselt number if the local quantities in Eq. (9) were replaced by average quantities, thus giving

$$\overline{\mathrm{Nu}}^n = \overline{\mathrm{Nu}}_F^n \pm \overline{\mathrm{Nu}}_N^n, \quad (10)$$

where the value of n used was 3. Note that the model had no need to handle the negative sign of Eq. (10). Each possible case scenario (i.e., heat flow up or heat flow down) was modeled separately; therefore, in all cases the forced convection and natural convection Nusselt numbers were additive. Nusselt number for external flow over a surface was calculated using

$$\overline{\mathrm{Nu}}_F = \frac{\bar{h}L}{k} = 0.664\ \mathrm{Re}^{1/2}\ \mathrm{Pr}^{1/3}$$

$$(\mathrm{Pr} \geq 0.6,\ \mathrm{Re} \leq 5 \times 10^5) \quad (11)$$

for laminar flow, and

$$\overline{\mathrm{Nu}}_F = (0.037\ \mathrm{Re}^{4/5} - 871)\ \mathrm{Pr}^{1/3}$$

$$(0.6 \leq \mathrm{Pr} \leq 60,\ 5 \times 10^5 \leq \mathrm{Re} \leq 10^8) \quad (12)$$

for turbulent flow. These correlations were used regardless of the orientation of the surface. However, different correlations in both laminar and turbulent regimes were used when dealing with natural convection depending on the surface orientation. Natural convection correlations vary for laminar or turbulent regimes and depend also on orientation as well as whether the surface is being heated or cooled. For a hot attic floor when losing heat to the ventilating air (summer and winter case), and for a cold ceiling being heated by the indoor air (winter), the following equations applied:

$$\overline{\mathrm{Nu}}_N = 0.54\ \mathrm{Ra}^{1/4} \quad (10^4 \leq \mathrm{Ra} \leq 10^7) \quad (13)$$

$$\overline{\mathrm{Nu}}_N = 0.15\ \mathrm{Ra}^{1/3} \quad (10^7 \leq \mathrm{Ra} \leq 10^{11}). \quad (14)$$

For a cold attic floor gaining heat (summer mornings), and for a hot ceiling losing heat to the indoor air (summer conditions),

$$\overline{\mathrm{Nu}}_N = 0.27\ \mathrm{Ra}^{1/4} \quad (10^5 \le \mathrm{Ra} \le 10^{10}). \tag{15}$$

Equations (11) through (15) were obtained from Incropera and DeWitt (1981). For the triangular end-gables regardless of heat flow direction, the following equation was applied (Churchill and Chu, 1975):

$$\overline{\mathrm{Nu}}_N = 0.68 + \frac{0.670\ \mathrm{Ra}^{1/4}}{\left[1 + \left(\frac{0.492}{\mathrm{Pr}}\right)^{9/16}\right]^{4/9}} (0 \le \mathrm{Ra} \le 10^9). \tag{16}$$

For the attic deck and roof sections which are neither horizontal nor vertical, the correlations (Peavy, 1979),

$$h_N = \frac{1.393(\Delta T)^{1/3}}{7.333 - \cos(\phi)}, \tag{17}$$

for heat flowing up, and

$$h_N = \frac{0.2613(\Delta T)^{1/3}}{1.375 + \cos(\phi)}, \tag{18}$$

for heat flowing down were used. In Eqs. (17) and (18), ΔT was the temperature difference between the surface and the air flowing next to it, and ϕ has the angle between the horizontal and the roof section. Under the forced ventilation arrangement (soffit/gable), it was assumed that ambient air entered the attic at a low point, flowed across the attic floor, and rose to the top of the attic (Fig. 2). This assumption is consistent with the fact that hotter air is lighter than colder air, and therefore, would rise, while colder air would travel along the floor of the attic.

The energy gained by the ventilating air as it traveled across the length of the attic floor was described by

$$\dot{m}C_p \frac{dT}{dx} = W_f h_{\mathrm{conv}}(T_f - T) \tag{19}$$

where W_f is the width of the attic. Equation (19) was rearranged to solve for the temperature of the attic air. It yielded

$$\int_{T_{\mathrm{ambient}}}^{T_{\mathrm{Low\ air}}} \frac{dT}{(T_f - T)} = \int_0^x \eta dx \tag{20}$$

where

$$\eta = \frac{W_f h_{\mathrm{conv}}}{\dot{m}C_p} \tag{21}$$

and $T_{\mathrm{Low\ air}}$ referred to the temperature of the attic air adjacent to the attic floor after the incoming air had traveled the entire distance of the attic length. This temperature was obtained from Eq. (20),

$$T_{\mathrm{Low\ air}} = T_f + (T_{\mathrm{ambient}} - T_f)e^{-\eta x}, \tag{22}$$

where T_{ambient} was the temperature of the entering air. Note that for the integration of Eq. (20) to be carried out, it was assumed that the convection coefficient (h) did not vary with distance along the length of the attic. The average air temperature of this air layer was calculated by integrating Eq. (22),

$$T_{\mathrm{Low\ air\ (avg)}} = \frac{1}{L}\int_{x=0}^{x=L} T_{\mathrm{Low\ air}} dx = T_f + \frac{(T_{\mathrm{ambient}} - T_f)}{\eta L}(1 - e^{-\eta L}), \tag{23}$$

and the maximum temperature was given by

$$T_{\mathrm{Low\ air\ (max)}} = T_f + (T_{\mathrm{ambient}} - T_f)e^{-\eta L}. \tag{24}$$

Moreover, attic air is usually stratified. Cold air flows along the bottom of the attic while hotter air flows along the top. To account for air stratification, the preceding derivation was extended to account for air traveling upward and flowing across the attic structure. Equation (19) was rewritten as

$$\dot{m}C_p \frac{dT_{\mathrm{air}}}{dy} = EW_{\mathrm{D1}}h_{\mathrm{conv\ D1}}(T_{\mathrm{D1}} - T_{\mathrm{air}}) + EW_{\mathrm{D2}}h_{\mathrm{conv\ D2}}(T_{\mathrm{D2}} - T_{\mathrm{air}}) + EW_{\mathrm{G1}}h_{\mathrm{conv\ G1}}(T_{\mathrm{G1}} - T_{\mathrm{air}}) + EW_{\mathrm{G2}}h_{\mathrm{conv\ G2}}(T_{\mathrm{G2}} - T_{\mathrm{air}}) \tag{25}$$

where EW referred to an "equivalent width" of attic components. Note that the equivalent width of the deck section was the length of the attic while the equivalent width of the end gables was the width of the gables. The subscripts D1 and D2 represent the deck section 1 and deck section 2, respectively. Similarly, subscripts G1 and G2 represented gable-end section 1 and gable-end section 2, respectively. The attic air temperature distribution at any level from the floor up was also developed

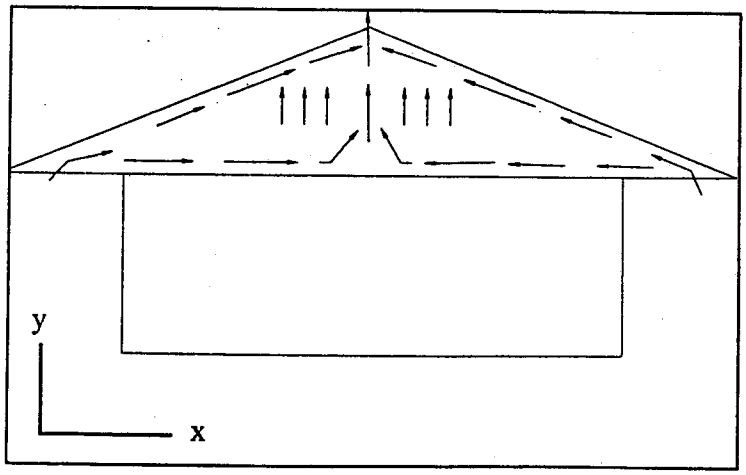

Fig. 2 Airflow pattern used in the simulation of attic ventilation

following the same analogy used in Eqs. (20)–(22), which resulted in

$$T_{\text{air}} = \frac{\lambda}{\iota} + \left(T_{\text{Low air (max)}} - \frac{\lambda}{\iota}\right)e^{-\iota y} \tag{26}$$

$$\iota = \eta_{D1} + \eta_{D2} + \eta_{G1} + \eta_{G2} \tag{27}$$

$$\lambda = \eta_{D1}T_{D1} + \eta_{D2}T_{D2} + \eta_{G1}T_{G1} + \eta_{G2}T_{G2} \tag{28}$$

$$\eta_* = \frac{EW_* h_{\text{conv}*}}{\dot{m}C_p} \tag{29}$$

where the asterisk, *, was replaced by the corresponding subscript (D1, D2, G1, or G2) for the corresponding section. The maximum attic air temperature (exit temperature) was given by

$$T_{\text{air(exit)}} = \frac{\lambda}{\iota} + \left(T_{\text{Lowair(max)}} - \frac{\lambda}{\iota}\right)e^{-\iota H} \tag{30}$$

where H was the distance from the top of the lower attic air layer to the bottom of the attic deck. The average attic temperature was then

$$T_{\text{air(avg)}} = \frac{\lambda}{\iota} + \frac{1}{H\iota}\left(T_{\text{Lowair(max)}} - \frac{\lambda}{\iota}\right)(1 - e^{-\iota H}). \tag{31}$$

Radiation Heat Transfer. Radiation heat transfer within the attic space was handled using radiation enclosure theory. The major assumptions were that attic surfaces were isothermal, gray, and diffuse. The gray-body assumption was a reasonable assumption because both the emitted and the incident radiation were confined to the same wavelength range (infrared), and in attics the spectral emittance is relatively constant within this range. The diffuse assumption required that all radiation emitted and reflected from any attic surface be diffusely distributed. In attic structures, both the emitted and reflected radiation are indistinguishable and there was no need to separate them. This assumption enabled the calculations to be based on radiosities. Radiosities are uniform along the surface when the surface is isothermal. The fact that radiosities are uniform along any attic surface made the view factors independent of the magnitude and surface distribution of the radiant energy flux. Attic radiation view factors were calculated from and to each surface. The calculations of attic view factors were performed for each surface by first setting $F_{i,i}$ equal to zero because there were no self-viewing surfaces. Second, the view factor between two flat rectangular planes having a common edge were calculated using the relation by Hamilton and Morgan (Hamilton and Morgan, 1952). The rest of the view factors were derived from view factor algebra. To be able to use the principles of matrix algebra as well as the restriction placed upon by the derivation of the response factors (boundary conditions must be linear), radiation heat transfer was approximated linearly. In the case of hour-by-hour simulation, the same enclosure had to be solved again and again for different sets of surface temperatures. Sparrow and Cess (1970) proposed a method in which the governing equations were solved only once, regardless of how many times the thermal boundary conditions were altered. The net radiation heat transfer flux between any two surfaces was calculated as follows (after Sparrow and Cess, 1970; Wilkes, 1991); starting with

$$\sum_{j=1}^{S} \chi_{i,j}B_j = \Omega_i \quad 1 \le i \le S \tag{32}$$

in which

$$\chi_{i,j} = \frac{\delta_{i,j} - (1 - \epsilon_i)F_{i,j}}{\epsilon_i} \tag{33}$$

and

$$\Omega_i = \sigma T_i^4 \tag{34}$$

$$\delta_{i,j} = \begin{cases} 1 & \text{if } i = j \\ 0 & \text{if } i \ne j \end{cases} \tag{35}$$

where B was the radiosity and S the number of surfaces. The coefficients $\chi_{i,j}$ and the term Ω_i were known constants (previous temperatures were used in Ω_i which were updated as the solution converged to new values of T). Upon evaluating Eq. (33) for surfaces, an S-by-S array of numbers was formed giving

$$\chi = \begin{vmatrix} \chi_{1,1} & \chi_{1,2} & \cdots & \chi_{1,s} \\ \chi_{2,1} & \chi_{2,2} & \cdots & \chi_{2,s} \\ \vdots & \vdots & & \vdots \\ \chi_{s,1} & \chi_{s,2} & \cdots & \chi_{s,s} \end{vmatrix} . \tag{36}$$

The inversion of matrix χ provided the matrix ψ

$$\psi = \chi^{-1} = \begin{vmatrix} \psi_{1,1} & \psi_{1,2} & \cdots & \psi_{1,s} \\ \psi_{2,1} & \psi_{2,2} & \cdots & \psi_{2,s} \\ \vdots & \vdots & & \vdots \\ \psi_{s,1} & \psi_{s,2} & \cdots & \psi_{s,s} \end{vmatrix} \tag{37}$$

and by employing the coefficients $\psi_{i,j}$, the following equations were written:

$$q''_{\text{rad}(i,j)} = H\ \text{rad}_{i,j}\ (T_i - T_j) \tag{38}$$

where

$$H\ \text{rad}_{i,j} = G_{i,j}\sigma(T_i^2 + T_j^2)(T_i + T_j) \tag{39}$$

and

$$G_{i,j} = \frac{\epsilon_i}{1 - \epsilon_i}\psi_{i,j} \tag{40}$$

where $H\ \text{rad}_{i,j}$ used previous values of temperatures. For the net radiation on the outer attic surfaces to the sky and surroundings, $H\ \text{rad}_{i,j}$ became

$$H\ \text{rad}_{i,\text{out}} = \epsilon_{i,\text{out}}\sigma(T_{i,\text{out}}^2 + T_{\text{sky/surr}}^2)(T_{i,\text{out}} + T_{\text{sky/surr}}), \tag{41}$$

where the subscripts "i, out" referred to the outer surface of surface i and $T_{\text{sky/surr}}$ referred to the temperature of the sky and/or surroundings. That is, it was assumed that the roof sections radiated to the sky while the end-gables radiated to the surroundings.

Solar Radiation on Attic Outer Surfaces. The driving force responsible for increasing the temperature of the shingles to a range of 65 to 75°C (~150 to 167°F) is solar radiation. This energy is eventually conducted through the roof sections and later radiated from the attic deck to the attic floor. Therefore, this is one of the major energy sources responsible for increasing the space cooling load of the residence. Radiant barrier systems have the potential of preventing most of this energy (from the attic deck) from being transferred to the attic floor. Solar radiation on attic surfaces (or "tilted" surfaces) is seldom measured, but the global radiation on a horizontal surface is measured at most weather stations around the country. The solar radiation on a horizontal surface was used to estimate the solar loads on inclined attic surfaces. Both the beam (or direct) component as well as the diffuse component were separated so that the direct component of global radiation could be multiplied to the respective angles describing the orientation of the surface and its relationship to the sun (Duffie and Beckman, 1980). To sepa-

rate these component, the load ratio of hourly diffuse to hourly total global radiation as well as the ratio of hourly total global radiation to hourly extraterrestrial radiation on a horizontal surface were estimated. All solar calculations were performed using true solar times using longitudes and standard meridians for the local time zones. The total radiation on an inclined surface was found, using

$$I_{\text{TILTED}} = I_d + R_b I_b \tag{42}$$

where

$$R_b = \frac{\cos(\theta)}{\cos(\theta_z)} \tag{43}$$

$$\begin{aligned}\cos(\theta) = {} & \sin(\delta)\sin(\phi)\cos(\beta) \\ & - \sin(\delta)\cos(\phi)\sin(\beta)\sin(\gamma) \\ & + \cos(\delta)\cos(\phi)\cos(\beta)\cos(\omega) \\ & + \cos(\delta)\sin(\phi)\sin(\beta)\cos(\gamma)\cos(\omega) \\ & + \cos(\delta)\sin(\beta)\sin(\gamma)\sin(\omega)\end{aligned} \tag{44}$$

and

$$\cos(\theta_z) = \sin(\delta)\sin(\phi) + \cos(\delta)\cos(\phi)\cos(\omega). \tag{45}$$

Net Sky Radiation From Attic Outer Surfaces. Infrared radiation heat transfer between attic outer surfaces and the sky is important during nighttime periods because under some conditions, this radiation can be the dominant mode of heat transfer. The study of infrared heat transfer between building surfaces and the sky, however, was handled using approximate relations because of the relative difficulty associated with obtaining accurate "sky data." The method used to calculate sky temperature was from Martin and Berdahl (1984) who calculated T_{sky} as follows:

$$T_{\text{sky}} = T_{\text{ambient}}[\epsilon_o + (1 + \epsilon_o)C]^{1/4} \tag{46}$$

$$\epsilon_o = 0.711 + 0.56\left(\frac{T_{dp}}{100}\right) + 0.73\left(\frac{T_{dp}}{100}\right)^2 + 0.13\cos\left[2\pi\frac{t}{24}\right] \tag{47}$$

$$C = n\epsilon_c\Gamma \tag{48}$$

where n is the fraction of the sky hemisphere covered by clouds and ϵ_c was the hemispherical cloud emissivity, and Γ a factor depending on the cloud base temperature.

Moisture Transport in Attic Structures. In humid climates, one of the major loads during the cooling seasons is from moisture transport. In winter, it is the condensation of moisture on the cold surfaces which creates changes in surface temperature and heat fluxes which cannot be estimated correctly under a "dry" air assumption. Moisture is also important in predicting degradation and deterioration of attic structures as well. Latent effects stem from various sources including moisture migration within structures, moisture transport by the ventilating air, as well as moisture adsorption/desorption at the interior surfaces. In this model, latent effects were incorporated in a steady-state fashion via a condensation/evaporation theory supplemented with suggestions from Burch et al. (1984), Cleary (1985), and Wilkes (1989). A steady-state moisture balance on the attic was written as

$$\sum_{\text{surface } i}^{S} A_i\,\text{Perm}_i\,(P_{o,i} - P_{\text{attic air}}) = \dot{Q}_{\text{air}}\rho_{\text{air}}(w_{\text{attic air}} - w_o) + \sum_{\text{surface } i}^{S} A_i h_{w,i}(w_{\text{attic air}} - w_{w,i}). \tag{49}$$

In Eq. (49), the first term on the left-hand side is the rate of moisture transfer by diffusion through the attic components. The first term on the right-hand side is the moisture transfer by exchange of attic air with the outdoor air and the last term is the moisture loss/gain by adsorption/desorption of water vapor at wood surfaces. Equation (49) can also be written in terms of $\omega_{\text{attic air}}$ as

$$\sum_{\text{surface } i}^{S} A_i\,\text{Perm}_i\,P_{\text{atm}}\left(\frac{w_{\text{attic air}}}{0.622 + \omega_{\text{attic air}}}\right) - P_{o,i} + \sum_{\text{surface } i}^{S} A_i h_{w,i}(w_{\text{attic air}} - w_{w,i}) + \dot{Q}_{\text{air}}\rho_{\text{air}}(w_{\text{attic air}} - w_o) = 0. \tag{50}$$

This expression was solved iteratively for $w_{\text{attic air}}$. In Eqs. (49) and (50) the mass transfer coefficient, $h_{w,i}$, was calculated using the Chilton-Colburn analogy (ASHRAE, 1989) between heat and mass transfer, the mass diffusivity term found in the Chilton-Colburn analogy was estimated using Sherwood's (1952) relation. In Eqs. (49) and (50), the wood humidity ratio was estimated using the following relation by Cleary (1985):

$$\begin{aligned} w_{w,i} &= e^{(Tsi/a)}(b + cu + du^2 + eu^3) \\ a &= 15.8°\text{C} \quad (28.6°\text{F}) \\ b &= -0.0015 \quad (-0.000498) \\ c &= 0.053 \quad (0.0172) \\ d &= -0.184 \quad (-0.060) \\ e &= 0.233 \quad (0.076) \end{aligned} \tag{51}$$

where u was the weight of water divided by the dry weight of wood. Once the attic air humidity ratio, the mass transfer coefficient, and the wood humidity ratio had been calculated, the latent load was obtained using

$$Q_{\text{latent}} = h_{w,i}(w_{\text{attic air}} - w_{w,i})h_{fg}, \tag{52}$$

where h_{fg} is the latent heat of vaporization of water.

Conclusions

This paper describes the development of a transient heat and mass transfer model. This model predicts hourly heat fluxes and surface temperatures in attic structures of residences. Further modifications must be made to accommodate retrofit cases. The model captures the relevant processes such as transient conduction, convection and radiation and incorporates others like moisture and air transport across the attic. Solar loads on outer attic surfaces and sky temperatures are also estimated. In addition, the model uses an attic air stratification pattern technique which is used to estimate attic air temperatures. The validation of the model with actual experimental data and simulations are presented in Part II of this paper.

References

ASHRAE, 1989, *Handbook of Fundamentals*, ASHRAE, Atlanta, GA.

Burch, D. M., Lemay, M. R., Rian, B. J., and Parker, E. J., 1984, "Experimental Validation of an Attic Condensation Model," *ASHRAE Transactions*, Vol. 20, Part 2A, pp. 59–77.

Chen, T. S., Armaly, B. F., and Ramachandran N., 1986, "Correlations for Laminar Mixed Convection Flows on Vertical, Inclined, and Horizontal Flat Plates," ASME *Journal of Heat Transfer*, Vol. 108, pp. 835–840.

Churchill, S. W., 1977, "A Comprehensive Correlating Equation for Laminar Assisting, Forced and Free Convection," *AIChE Journal*, Vol. 23, pp. 10–16.

Churchill, S. W., and Chu, H. H. S., 1975, "Correlating Equations for Laminar and Turbulent Free Convection from a Vertical Plate," *International Journal of Heat and Mass Transfer*, Vol. 18, p. 1323.

Cleary, P. G., 1985, "Moisture Control by Attic Ventilation—An In-Situ Study," *ASHRAE Transactions*, Vol. 91, Part 1, pp. 227–239.

Duffie, J. A., and Beckman, 1974, *Solar Thermal Energy Processes*, John Wiley and Sons, New York.

Hamilton, D. C., and Morgan, W. R., 1952, "Radiant Interchange Configuration Factors," NACA TN 2836.

Incropera, F. P., and Dewitt, D. P., 1981, *Fundamentals of Heat Transfer*, John Wiley and Sons, New York.

Martin, A., and Berdahl, 1984, "Characteristics of Infrared Sky Radiation in the United States," *Solar Energy*, Vol. 33, pp. 321–336.

Mitalas, G. P., and Stephenson, D. G., 1967, "Room Thermal Response Factors," *ASHRAE Transactions*, Vol. 73, Part I.

Peavy, B. A., 1979, "A Model for Predicting the Thermal Performance of Ventilated Attics," *Summer Attic and Whole House Ventilation*, NBS SP 548, Washington D.C.

Sherwood, T. K., and Pigford, R. L., 1952, *Absorption and Extraction*, McGraw-Hill, New York.

Sparrow, E. M., and Cess, R. D., 1970, *Radiation Heat Transfer*, Brooks/Cole Publishing Co., Belmont, CA.

Wilkes, K. E., 1989, "Modeling of Residential Attics with Radiant Barriers," *Proceedings of the Fifth Annual Symposium on Improving Building Energy Efficiency in Hot and Humid Climates*, Houston, TX, pp. 161–168.

Wilkes, K. E., 1991, "Analysis of Annual Thermal and Moisture Performance of Radiant Barrier Systems," ORNL/CON-319, Oak Ridge National Laboratory, Oak Ridge, TN.

APPENDIX

Estimation of X_o, X_1, Y_o, and Y_1 was performed using the following equations:

$$X_o = -\frac{k}{l}\frac{l^2}{\alpha\Delta}\left[\frac{\alpha n\Delta}{l^2} - \frac{1}{3} + \frac{2}{\pi^2}\sum_{m=1}^{\infty}\frac{\gamma_m}{m^2}\right]$$

$$X_1 = -\frac{k}{l}\frac{l^2}{\alpha\Delta}\left[\frac{1}{3} + \frac{2}{\pi^2}\sum_{m=1}^{\infty}\frac{\gamma_m^2 - 2\gamma_m}{m^2}\right]$$

$$Y_o = -\frac{k}{l}\frac{l^2}{\alpha\Delta}\left[\frac{1}{6} - \frac{\alpha\Delta}{l^2} + \frac{2}{\pi^2}\sum_{m=1}^{\infty}\frac{(-1)^m\gamma_m}{m^2}\right]$$

$$Y_1 = -\frac{k}{l}\frac{l^2}{\alpha\Delta}\left[-\frac{1}{6} + \frac{2}{\pi^2}\sum_{m=1}^{\infty}\frac{(-1)^m(\gamma_m^2 - 2\gamma_m)}{m^2}\right].$$